Journal of
Renewable Energy Research and Applications (RERA)

Vol. 3, No. 2, 2022, 217-228 *DOI: 10.22044/rera.2022.11508.1095*

Sensitivity Analysis in a Multi-Carrier Energy Hub System Through Electrical and Thermal Profile Procurement

M. Mahmoudian, S. Sadi*, J. Gholami and A. Karimi

Department of mechanical engineering, Imam Hossein Comprehensive University.

Receive Date 21 December 2021; Revised Date 15 January 2022; Accepted Date 12 February 2022
Corresponding author: m.mahmoudian@sutech.ac.ir (M. Mahmoudian)

Abstract
This work deals with the energy hub systems in order to evaluate the sensitivity analysis of the output power carriers in terms of the input electricity and natural gas. Unlike the recent works that have solitary concentrated on the operational cost minimization, in this research work, not only the energy carriers of the proposed hub are being modeled but also the sensitivity analysis of each power supplier is investigated. Since some of the input power carriers in the hub are decreased slightly or immediately according to the unsolicited situations, the output electrical or thermal profile may not be supplied completely. Therefore, the network operator must make a proper decision in order to utilize the best carriers not to reduce the system efficiency, if possible. In this regard, the objective function including the energy costs for the electrical, thermal, and cooling demand carriers is optimized, and the best solution is extracted based on the conditional value at risk (CAVR) of the electricity market actors using the GAMS/CPLEX software. According to the results obtained, the higher the risk that the network operator takes, the higher the profit from the future contracts. In the next step, the electricity price is predicted using the ARIMA approach for the next four weeks, and the sensitivity analysis for the future of the energy hub is examined. The simulation results and the changes in the share of energy carriers show that the importance of passive defense must be considered in planning for the energy supply of the office buildings, and the percentage of the unsupplied energy must be studied.

Keywords: *Energy Hub, Electricity Market, Conditional Value at Risk, Optimization, Sensitivity Analysis.*

1. Introduction

An energy hub system consists of some power carriers with different performances that are integrated together within the coherent operation preservation. Power supplement for energy is required in the commercial, residential, and the industrial loads result in the development in generation of expansion planning [1]. Since the electrical power and natural gas with their interaction through combined heat and power (CHP) devices, electric heat pumps (EHPs), etc. increase the synergy, the system efficiency will growth up correspondingly [2]. This issue is achieved by providing a basis to feed the demand load within a semi-lossless energy hub system. Inside the general hubs, regularly, there are transformers, power electronic interfaces, compressors, thermal exchangers and combined cooling heat and power (CCHP), and some converters, as shown in Figure. 1. Many research works have been conducted so far on optimal energy hub operation considering the cost minimization. Most of them concentrate on the CHP programing and unit commitment. The energy hub concept or multi-carrier energy system performance has recently been introduced by the novel researchers [3].

The authors in [4] have provide a framework for modeling and optimizing the systems with multiple energy carriers. Based on the concept of energy hub, a sustainable model for converting and storing the multiple energy carriers such as electricity, natural gas, hydrogen, and local heat has been used to optimize the system. The modeling method for using the multiple energy carrier systems inside the buildings is based on the concept of energy hub in [5]. This method allows modeling of energy coupling between the energy supply sources and the desired loads in the combined methods. The authors in [6] have delivered a model of an energy hub with CHP and wind turbine and solar cell and a water electrolyzer in order to produce hydrogen. In all

the above references, attention to the network requirements such as the inlet gas pressure to the hub and bus voltage has not been considered, and the hub has been examined and designed independently from the network. The design and determination of the optimal capacity of the interconnected hubs by considering the physical constraints in the electricity and gas networks and environmental issues have been presented in [7]. The authors in [8] have presented a new method for planning and developing the distribution system production with the concept of energy hub. The proposed algorithm divides the problem into several sub-problems in order to minimize the investment and operating costs, while improving the reliability. The authors in [9] have dealt with the long-term planning of the six-bus electricity and natural gas network. This reference has tried to solve the objective function through the linear programming method by the linearizing relations. The above articles also pay attention to the design and long-term planning of the hub, while the purpose of this article is to schedule the operation of the micro-grid for the day ahead. The authors in [10] have investigated the issues of equipment efficiency and uncertainty of power, and price and electrical load are included in the optimization problem. The authors in [11] have proposed a residential energy hub for a smart home. A residential CHP and an electric vehicle are included in the model, and the energy consumed and how to convert it inside the hub. A robust optimization method to solve the problem of optimizing the operation of an energy hub has been presented in [12]. In fact, in this article, the amount of energy purchased and stored has been optimally obtained. The authors in [13] have dealt with the objective function, and have maximized the profit of the owner of the energy hub by considering the risk of uncertainties.

In the same way, the authors in [14] have presented a new framework to solve the load flow equations in the energy hub space. The inputs and outputs are related together with high-order matrices that make the problem formulation completely non-linear so that the robust optimization approach is hired to solve the objective function. The authors in [15] have presented a mathematical model of CHP equipment in the low-scale optimization but the operation cost does not contain the other interchanges among the energies wasted there. In [16], a linear programing (LP) approach has been hired in order to minimize the operation costs in the presence of CHP. However, no sensitivity analysis has been figured out. An optimal problem formulation has been expressed in [17] in order to minimize the operation costs of the multi-carrier power system. The optimization problem is based on the multi-parametric genetic algorithm (GA), which divides the main fitness function into some sub-problem equations. Therefore, the least disturbances are crashed to the energy hub system; nevertheless, no time saving for the objective function solving has yet been presented. The authors in [9] have presented a model to program the wind farm in the presence of CHPs, and then in [18], this mathematical formulation has been completed considering the instantaneous operation of photovoltaic (PV) system and energy management system (EMS). In any case, no sensitivity analysis has been obtained in both the above-mentioned works.

The renewable energy resource) performance in the multi-carrier energy systems is always self-challenging. Likewise, the authors in [19] have evaluated the economic dispatch (ED) problem in the presence of wind turbine (WT). The uncertainties appearing in the wind performance will make this problem to be probabilistic ED. This paper also tries to determine the share of each energy carrier in order to obtain the best controllability and visibility. In [20], the power generated by WTs is being management with the purpose of minimizing the objective function. The robust optimization strategy will result in reduced operation costs but the wind uncertainties have not been paid attention to. In [21], the authors have solved the energy hub optimization using the LP approach, while the decision vectors and control parameters have been considered as the energy purchased and sold during a day. There have been some efforts to investigate the EMS and battery energy storage system (BESS) but some restrictions on hydrogen procurement have made these research works unfinished. The authors in [22] have presented a new concept to energy hub named economic valuation, which measures the worthiness of the natural gas, heat exchangers, and electricity price. In fact, the electric power or the natural gas purchased form the electricity market and heat market, respectively, should be valuated before utilization. Then the ED solution is achieved within ignoring the sensitivity analysis.

The authors in [23] have proposed an energy management framework with heat evaluation based on the electricity purchased and consumed in the residential loads. However, they have not mentioned RESs. Unlike that, the others in [24] have much paid attention to the plug-in electric vehicle (PEV) operation with RES influences. The

significance of this novelty is to consider the reactive power compensation in the electric distribution network according to the PEV travels. PEVs have the capability to inject the reactive power into the non-compensated nodes in order to improve the voltage profile, as the static VAR commentator (STATCOM) does.

In this paper, the considered energy hub includes the electricity distribution network, natural gas, CHP, EHP, furnace, and chiller boiler (CB) to supply all the power demands. Therefore, the system modeling is completely formulated with a mathematical foundation. Then the multi-objective function describing the operation cost and sensitivity utility is presented in the next section. The most useful novelty of the conducted work is listed below:

- Sharing determination of the input energy carriers in terms of the parameter variations.
- The CVaR variable will impact on the ISO optimal decision-making.
- Energy not supplied is evaluated through the sensitivity process.
- Electricity price forecasting is considered since it highly impresses the problem formulation.

The nomenclature used in this paper is written below.

Nomenclature

α	Confidence level
β	Trade-off number between risk and cost
η	Positive axillary variable based in scenario
μ	Positive axillary variable
COP	Coefficient of performance for EHP
h_t	Binary variable for EHP heat power
c_t	Binary variable for EHP cooling power
w_t	Binary variable for CHP SU/SD cost
C_{SU}^{CHP}	Total start-up cost for CHP
SU_j^{CHP}	Start-up cost for CHP at jth block
C_{SD}^{CHP}	Total shut-down cost
SD_j^{CHP}	Shut-down cost for CHP at jth block
$k_{t,j}^{CHP}$	Binary variable for CHP commitment
γ_e^{CHP}	Percentage of generated electrical power
b_t	Binary variable for CB commitment
η_{CB}	Efficiency of CB
$\gamma_e^{furnace}$	Percentage of generated thermal power
$P_{t,l}^{gas(input,F)}$	Input natural gas power for furnace
P_{CD}	Cooling power demand
$P_{CD,EHP}$	Cooling power generated by EHP
$P_{CD,CB}$	Cooling power generated by CB
P_{HD}	Heat power demand
$P_{HD,EHP}$	Heat power generated by EHP
H^{CHP}	Heat power generated by CHP
$H^{Furnace}$	Heat power generated by furnace
P_{ED}	Electrical power demand
P_{EG}	Grid electrical power
$P_{t,j}^{elec(CHP)}$	CHP electrical power at jth block at time *t*
P^{CHP}	Total CHP generate power
$P_{t,j}^{gas(CHP)}$	CHP thermal power at jth block at time *t*
η_{Tr}	Transformer efficiency

2. Problem Formulation

A sample integrated electricity and gas grid is shown in figure 1, and the equivalent energy hub configuration under consideration of that is represented in figure 2. As shown, the input power carriers include the electrical energy purchased form the electricity distribution network and natural gas purchased from the heat grid. The outputs contain the electrical and thermal load demand within the cooling power that must procure separately. The interaction energy will be done among the electrical transformer, CHP, EHP, furnace, and CB.

The BESS is excluded in the proposed system due to the expensive operation cost.

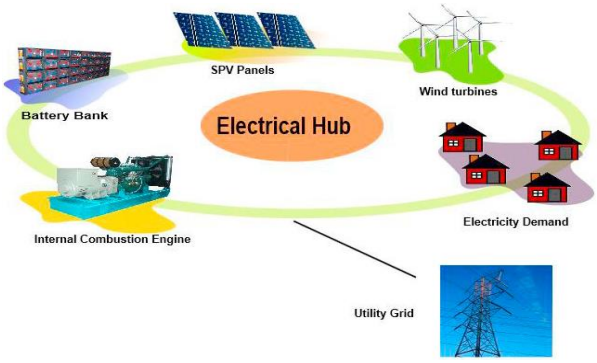

Figure 1. A typical energy hub system.

In order to evaluate the operation cost in the first step, the mathematical formulation of all equipment should be extracted.

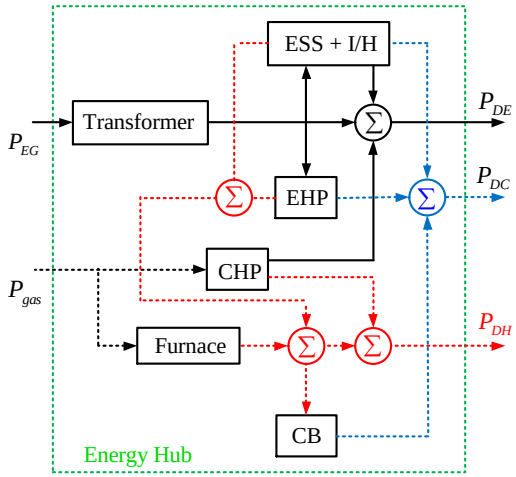

Figure 2. Block diagram of proposed energy hub.

2.1. CHP modeling

In the CHP operation, the heat power can be estimated piecewise linear in accordance with the efficiency and loading percentage. Since CHP can generate electrical and thermal power instantaneously, the total electricity produced can be calculated by (1) to (3) [5].

$$\mathbf{P^{CHP}} = \sum_{t=1}^{\hat{} } \sum_{j=1}^{\cdots} \boldsymbol{\gamma}_{e}^{\mathbf{CHP}} * \mathbf{P}_{t,j}^{\mathbf{gas(CHP)}} \quad (1)$$

$$\mathbf{P}_{t,j-1}^{\mathbf{elec(CHP)}} * \mathbf{k}_{t,j}^{\mathbf{CHP}} < \mathbf{P}_{t,j}^{\mathbf{CHP}} < \mathbf{P}_{t,j}^{\mathbf{elec(CHP)}} * \mathbf{k}_{t,j}^{\mathbf{CHP}} \quad (2)$$

$$\sum_{j=1}^{\cdots} \mathbf{k}_{t,j}^{\mathbf{CHP}} = \mathbf{1} \quad (3)$$

The electricity power generated from the input natural gas was determined by γ_e^{CHP}. The remaining power will be converter to the heat demand. Eq. (2) relies on that the CHP generated power must be exactly between the previous one and the next one. This power must be extracted from one block of the CHP characteristics, merely, which is proved by (3). The heat power generated by CHP can be mathematically formulated as follows in (4) [5].

$$\mathbf{H^{CHP}} = \sum_{t=1}^{T} \sum_{j=1}^{N_{CHP}} \boldsymbol{\gamma}_{g}^{\mathbf{CHP}} * \mathbf{P}_{t,j}^{\mathbf{gas(CHP)}} \quad (4)$$

while the turn-on and turn-off costs of that should have been considered in (5) and (6), respectively [6].

$$\mathbf{C_{SU}^{CHP}} = \mathbf{SU_j^{CHP}} * \mathbf{w_t}(\mathbf{1} - \mathbf{w_{t-1}}) \quad (5)$$

$$\mathbf{C_{SD}^{CHP}} = \mathbf{SD_j^{CHP}} * \mathbf{w_{t-1}}(\mathbf{1} - \mathbf{w_t}) \quad (6)$$

It should be noted that a convex area for the best performance of CHP must be considered as Figure 3 in order to confirm the relations between the heat and the electrical power; otherwise, the solution obtained from the optimization problem may be wrong. Therefore, the constraints below will be added to the objective function to represent the CHP performance areas [6].

$$\mathbf{P^{CHP}} - \mathbf{P_A^{CHP}} - \frac{\mathbf{P_A^{CHP}} - \mathbf{P_B^{CHP}}}{\mathbf{H_A^{CHP}} - \mathbf{H_B^{CHP}}} * \left(\mathbf{P^{CHP}} - \mathbf{P_A^{CHP}}\right) < \mathbf{0} \quad (7)$$

$$\mathbf{P^{CHP}} - \mathbf{P_B^{CHP}} - \frac{\mathbf{P_B^{CHP}} - \mathbf{P_C^{CHP}}}{\mathbf{H_B^{CHP}} - \mathbf{H_C^{CHP}}} * (\mathbf{P^{CHP}} - \mathbf{P_B^{CHP}}) > \mathbf{0} \quad (8)$$

$$\mathbf{P^{CHP}} - \mathbf{P_C^{CHP}} - \frac{\mathbf{P_C^{CHP}} - \mathbf{P_D^{CHP}}}{\mathbf{H_C^{CHP}} - \mathbf{H_D^{CHP}}} * (\mathbf{P^{CHP}} - \mathbf{P_C^{CHP}}) > \mathbf{0} \quad (9)$$

The horizontal axis of the diagram shown in Figure 3 determines the thermal power, and the vertical axis represents the electrical power generated. Equation 7 specifies all the surfaces under the line AB. Also equation 8 and equation 9 define all the areas upper than the lines BC and CD, correspondingly. The subscription of these three areas represents the permissible range of the CHP performance.

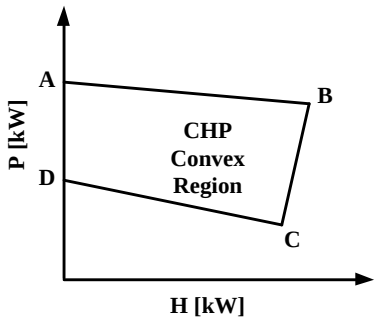

Figure 3. CHP convex region [6].

2.2. EHP formulation

An EHP device consumes electrical energy, and generates the cooling power or thermal power depending on the operation mode. EHP is out of work, while Eq. (13) satisfies the zero. The operation principles of EHP are mathematically formulated as follow [6]:

$$\mathbf{P_{CD,EHP} + P_{HD,EHP} = P_{EG,EHP} \times COP} \tag{10}$$

$$\mathbf{P^{min}_{HD,EHP}.h_t < P_{HD,EHP} < P^{max}_{HD,EHP}.h_t} \tag{11}$$

$$\mathbf{P^{min}_{CD,EHP}.c_t < P_{CD,EHP} < P^{max}_{CD,EHP}.c_t} \tag{12}$$

$$\mathbf{c_t + h_t \leq 1} \tag{13}$$

2.3. CB modeling

In the CB equipment, the cooling power is generated in terms of the heat power received. Due to its efficiency, the mathematical formulation of the CB operation is described as (14) [12].

$$\mathbf{P_{CD,CB} = b_t.\eta_{CB}.P_{HD,CB}} \tag{14}$$

2.4. Furnace modeling

In order to procure the thermal load profile directly, the furnace is utilized. This device receives the natural gas, and produces heat power, which is formulated as (15) [13-14].

$$\mathbf{H^{Furnace}} = \sum_{t=1}^{T} \sum_{l=1}^{N_{furnace}} \gamma_e^{furnace} * P_{t,l}^{gas(input)} \tag{15}$$

2.5. Energy storage modeling and ice-making

In this work, in order to increase the reliability of the electric power procurement, a set of energy storage was considered in order to improve the grid performance. Therefore, the electricity storage device (battery), heat storage device, and cooling energy device (ice storage tank) were, respectively, subjected to (16)–(18). It is worth mentioning that the charging cooling energy device is just the ice-making capacity, and the discharging cooling energy is just the ice-melting capacity. Besides, the ice-making and ice-melting modes cannot operate simultaneously [25].

$$\begin{aligned}
&\mathbf{E^{t+1}_{es} = E^t_{es}(1-\delta_{es}) + \Delta t\left(P^t_{es,c}\eta_{es,c} - \frac{P^t_{es,d}}{\eta_{es,d}}\right)}\\
&\mathbf{0 < P^t_{es,c} < u_{es}P^{max}_{es,c}}\\
&\mathbf{0 < P^t_{es,d} < (1-u_{es})P^{max}_{es,d}}\\
&\mathbf{E^{min}_{es} < E^t_{es} < E^{max}_{es}}
\end{aligned} \tag{16}$$

$$\begin{aligned}
&\mathbf{E^{t+1}_{hs} = E^t_{hs}(1-\delta_{hs}) + \Delta t\left(P^t_{hs,c}\eta_{hs,c} - \frac{P^t_{hs,d}}{\eta_{hs,d}}\right)}\\
&\mathbf{0 < P^t_{hs,c} < u_{hs}P^{max}_{hs,c}}\\
&\mathbf{0 < P^t_{hs,d} < (1-u_{hs})P^{max}_{hs,d}}\\
&\mathbf{E^{min}_{hs} < E^t_{hs} < E^{max}_{hs}}
\end{aligned} \tag{17}$$

$$\begin{aligned}
&\mathbf{E^{t+1}_{cs} = E^t_{cs}(1-\delta_{cs}) + \Delta t\left(P^t_{cs,c}\eta_{cs,c} - \frac{P^t_{cs,d}}{\eta_{cs,d}}\right)}\\
&\mathbf{0 < P^t_{cs,c} < u_{cs}P^{max}_{cs,c}}\\
&\mathbf{0 < P^t_{cs,d} < (1-u_{cs})P^{max}_{cs,d}}\\
&\mathbf{E^{min}_{cs} < E^t_{cs} < E^{max}_{cs}}
\end{aligned} \tag{18}$$

where the indices *e*, *h*, and *c* represent the electric energy, heat transferring, and cooling power exchanging in energy hub. E and $P^t_{cs,c}$ are the energy and the electric power used to supply the hub, while δ and u are the binary variables that imply the turn on/off devices.

2.6. CVaR

In a perfect and competitive market, the risk plays an important role in the quality evaluation of the generation units. Risk measurement always requires some powerful instrumentation to be calculated. For example, the value at risk (VaR) is introduced as a significant criterion, and determines a unique value. In [15], VaR and CVar are mathematically formulated as the following equations.

$$\mathbf{VaR = Max\{x|(profit < x) < 1-\alpha\}} \tag{19}$$

$$\mathbf{CVaR = Expexted\{profit|profit < VaR\}} \tag{20}$$

The confidence or reliability level (α) is usually selected to be 0.95. Therefore, the CVaR formulation is completed within (21) [16].

$$\mathbf{CVaR} = \sum_{t=1}^{T} \beta\left(\zeta - \frac{1}{1-\alpha}\sum_{i=1}^{N_i}\eta(t,i).\mu(t,i)\right) \tag{21}$$

subject to:

$$\begin{aligned}
&\mathbf{-profit(i) + \zeta - \eta(t,i) < 0 \;\; ; \;\; \forall i = 1,2,\dots,N_i}\\
&\mathbf{\eta(t,i) > 0 \;\; ; \;\; \forall i = 1,2,\dots,N_i}
\end{aligned} \tag{22}$$

3. Objective Function

The optimization problem is to solve the equation written in (23) in order to minimize the total operation cast (OC) of the multi-carrier energy hub system containing the cooling heat and

power, electric heat pump, cooling boiler, furnace, energy storage with ice-making, and risk management of the operator decisions. Due to the unchanging of the load profile in the hub outputs, the only factors to be optimized will be the power purchased and the interaction process cost.

$$\mathbf{OC} = \sum_{t=1}^{T} \boldsymbol{\pi}_{\mathbf{EG}}(\mathbf{t}) \,.\, \mathbf{P}_{\mathbf{EG}}(\mathbf{t}) + \sum_{t=1}^{T} \boldsymbol{\pi}_{\mathbf{gas}}(\mathbf{t}) \,.\, \mathbf{P}_{\mathbf{gas}}(\mathbf{t}) + \mathbf{SU}_{\mathbf{m}}^{\mathbf{DG}} . \mathbf{u}_{\mathbf{t}} + \mathbf{SD}_{\mathbf{m}}^{\mathbf{DG}} . \mathbf{u}_{\mathbf{t-1}} + \mathbf{SU}_{\mathbf{j}}^{\mathbf{CHP}} . \mathbf{w}_{\mathbf{t}} + \mathbf{SD}_{\mathbf{j}}^{\mathbf{CHP}} . \mathbf{w}_{\mathbf{t-1}} \quad (23)$$

$$1. + \sum_{t=1}^{T} \boldsymbol{\beta} \left(\boldsymbol{\zeta} - \frac{1}{1-\alpha} \sum_{i=1}^{N_i} \boldsymbol{\eta}(\mathbf{t}, \mathbf{i}) . \boldsymbol{\mu}(\mathbf{t}, \mathbf{i}) \right).$$

while the equality and non-equality constraints are expressed in (24)–(27) [8].

3.1. Cooling demand criteria

$$\mathbf{P}_{\mathbf{CD,EHP}} + \mathbf{P}_{\mathbf{CD,CB}} + \mathbf{P}_{\mathbf{CD,ICE}} = \mathbf{P}_{\mathbf{CD}} \quad (24)$$

3.2. Thermal demand criteria

$$\mathbf{P}_{\mathbf{HD,EHP}} + \mathbf{H}^{\mathbf{CHP}} + \mathbf{H}^{\mathbf{Furnace}} + \mathbf{P}_{\mathbf{HD,ESS}} = \mathbf{P}_{\mathbf{HD}} \quad (25)$$

3.3. Electrical demand criteria

$$\mathbf{P}_{\mathbf{t,j}}^{\mathbf{elec(CHP)}} + \boldsymbol{\eta}_{\mathbf{Tr}} \mathbf{P}_{\mathbf{EG}} + \mathbf{P}_{\mathbf{E,ESS}} = \mathbf{P}_{\mathbf{ED}} \quad (26)$$

3.4. Non-equality constraints

$$\begin{aligned}
&H^{CHP,max} < H^{CHP} < H^{CHP,min} \\
&P_{t,j}^{elec(CHP),min} < P_{t,j}^{elec(CHP)} < P_{t,j}^{elec(CHP),max} \\
&H^{Furnace,max} < H^{Furnace} < H^{Furnace,min} \\
&P_{CD,EHP}^{min} < P_{CD,EHP} < P_{CD,EHP}^{max} \\
&P_{HD,EHP}^{min} < P_{HD,EHP} < P_{HD,EHP}^{max} \\
&P_{E,ESS}^{min} < P_{E,ESS} < P_{E,ESS}^{max} \\
&P_{H,ESS}^{min} < P_{H,ESS} < P_{H,ESS}^{max} \\
&P_{CB,ICE}^{min} < P_{CB,ICE} < P_{CB<ICE}^{max} \\
&0 < \alpha < 1
\end{aligned} \quad (27)$$

4. Short-term Electricity Price Forecasting

The Auto-Regressive and Integrated Moving Average (ARIMA) time series model can be used with the variable mean or variance values [26]. This method uses the historical data in order to forecast the future data. The method that was applied in this work to predict the electricity market prices was based on [27]. If the electricity market prices are represented by λ_t, then a generic ARIMA model is as follows:

$$\boldsymbol{\phi}(\mathbf{B})\boldsymbol{\lambda}_{\mathbf{t}} = \boldsymbol{\phi}(\boldsymbol{\theta})\boldsymbol{\varepsilon}_{\mathbf{t}} \quad (28)$$

where $\phi(B)$ and $\phi(\theta)$ are the back-shift operators, and ε_t represents the normal white noise. These are obtained using the Box and Jenkins method using the auto-correlation and partial auto-correlation functions. The historical price data of three weeks in the electricity market was used to forecast the electricity market prices in the future. The auto-correlation and partial auto-correlation functions are shown in figure 4.

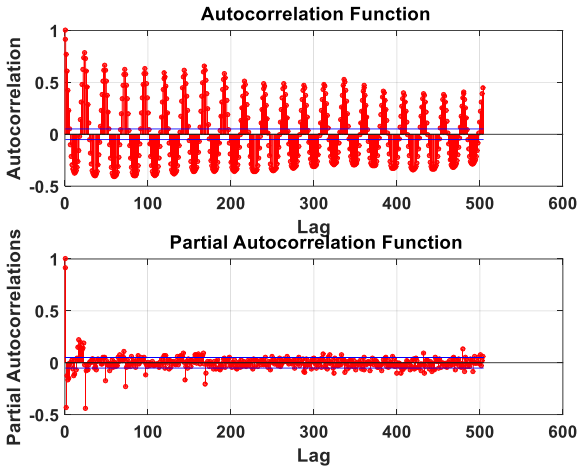

Figure 4. Auto-correlation and partial auto-correlation coefficients.

Then the resulting ARIMA time series model is:

$$\begin{aligned}
&(\mathbf{1} - \mathbf{0.032\ B_1}) * (\mathbf{1} + \mathbf{0.125\ B_2} - \mathbf{0.745\ B_3}) * \\
&(\mathbf{1} - \mathbf{0.245\ B_7} + \mathbf{0.552\ B_{11}}) * (\mathbf{1} - \mathbf{B_{13}}) * \\
&(\mathbf{1} - \mathbf{0.142\ B_{21}}) * \mathbf{log}(\boldsymbol{\lambda}_{\mathbf{t}}) = (\mathbf{1} + \mathbf{0.625\ B_2}) * \\
&(\mathbf{1} - \mathbf{0.845\ B_7} - \mathbf{0.542\ B_{14}} + \mathbf{0.985\ B_{20}})
\end{aligned} \quad (29)$$

The mean absolute percentage error is calculated in (30) so that the forecasted electricity price is represented in figure 5. The upper band and lower band will guarantee the prediction areas [27].

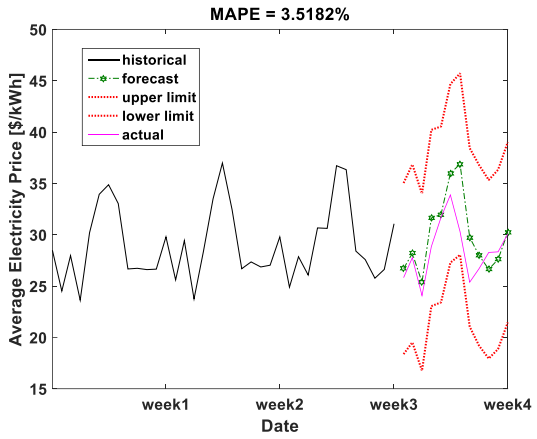

Figure 5. Predicted electricity price.

$$\mathbf{MAPE} = \frac{\mathbf{1}}{\mathbf{N}} \sum_{\mathbf{i=1}}^{\mathbf{N}} \left| \frac{\mathbf{Price_i - Price_{ave}}}{\mathbf{Price_{ave}}} * \mathbf{100} \right| \% \qquad (30)$$

5. Simulation Results in Base Case

The objective function described in the previous sections is now being minimized to obtain the best solution through the equality and non-equality constraints. In this case, the energy not supplied (ENS) was calculated as zero. There are three load profiles that should be supplied by the electricity and natural gas energies purchased from the upstream network: electrical demand, thermal profile, and cooling load. The electrical demand in the base case will be procured using CHP, EHP, ESS, and grid power.

Similarly, the thermal profile is supplied by CHP, furnace, and battery heating power, and the last one, the cooling load, is supplied by CB and ice-making power extracted from the battery equipment. The simulation results represent these load profile procurement in figures 6 to 8.

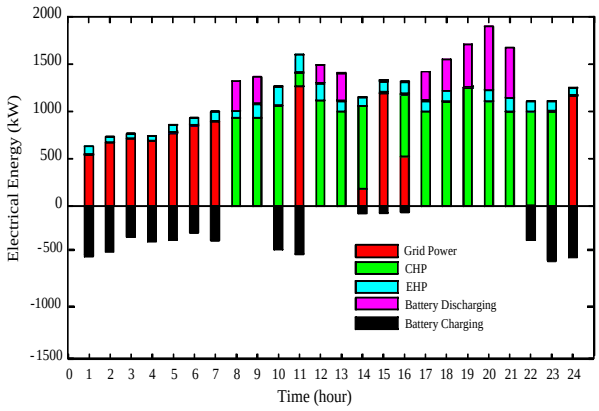

Figure 6. Electrical demand procurement.

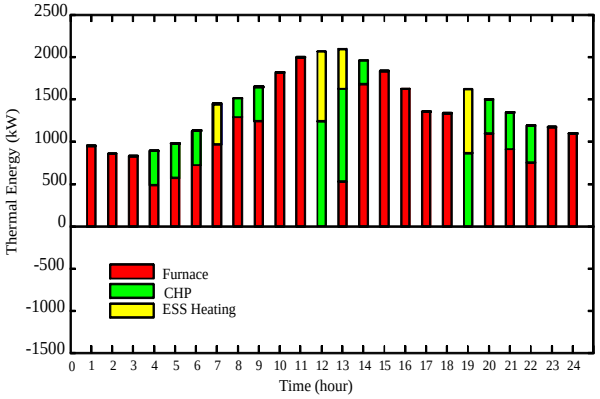

Figure 7. Thermal demand procurement.

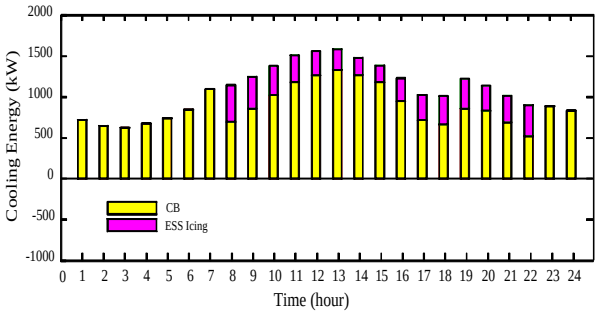

Figure 8. Cooling demand procurement.

Figure 6 shows that the energy purchased from the upstream grid that will be cost-effective in the event of a light load interval, and when the electricity tariff increases, CHP will also contribute to generate the electrical power. In the peak load periods, the battery is discharged and helps the power carriers to provide the required demand. It is worth noting that in the times of light load conditions, the battery is also charged (black chart) to reduce the total cost of the operation. In this regard, EHP takes a small share of the power supply due to its low capacity. From figure 7, which shows the share of energy carriers to provide thermal demand, it can be concluded that the furnace has the highest share in most hours of the day, and only a small amount of power of CHP and ESS have been used. These interpretations are also applied to figure 8, meaning that most of the cooling power is provided by CB, and e ESS will only enter the circuit during the peak hours.

6. Sensitivity Analysis

The time horizon of the simulations was considered as 24 hours a week, and the mathematical formulations were solved in the GAMS platform. In the base case simulation, no contingency happened so that the total load power (electric, thermal, and cooling) were completely supplied by the energy sources. In this section, the

sensitivity analysis of the power outage of energy sources is investigated as decreasing steeply.

6.1. CHP outage

Imagine that CHP is crashed due to the power oscillations or an interruption in the transmission gas lines. Thus CHP is going to be out of the circuit with the steps 30%, 50%, and 100% so that the electricity produced by CHP is substituted with ESS, the grid power, and EHP. Likewise, the gas not supplied should have been provided by the furnace and ESS heating devices. Table 1 represents the CHP outage effects on the electrical and thermal load procurement, which influence the other energy sources. Figure 9 represents the operation costs and ENS in terms of the CHP outage. As it can be observed, the operation costs are increasing since the CHP outage level rises as well. ENS in all the sensitivity analysis sections are increased, while the energy sources will be out of the circuit, correspondingly.

Table 1. Energy surplus percentage of energy sources in CHP outage rather than base case.

Energy sources	CHP outage percentage		
	30%	50%	100%
EHP	1.12%	1.23%	1.44%
CB	1.04%	1.09%	1.13%
Furnace	1.13%	1.17%	1.26%
ESS	1.16%	1.22%	1.43%

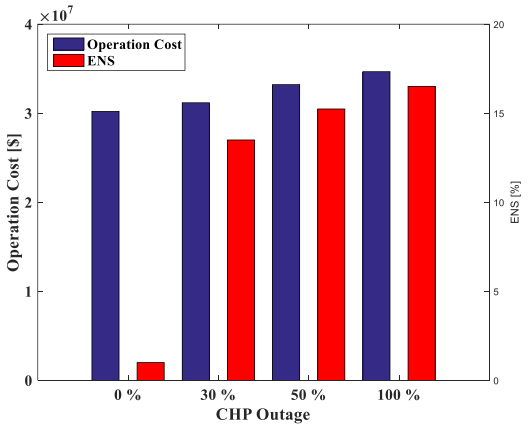

Figure 9. Operation costs and ENS in terms of CHP outage.

Since CHP is the largest and most expensive equipment in the energy hub, its outage can have a more dangerous impact on the system stability. Figure 9 also shows that the operating costs have increased about $5 million, and ENS has reached about 16%, which can be a serious threat to the system demand procurement. Therefore, paying attention to the passive defense in energy hub planning will be very decisive.

6.2. EHP outage

Since the EHP power source steps out of the circuit, the other energy sources are influenced, accordingly. Table 2 and figure 10 show the effects of EHP outage on the surplus energy produced and the operation costs. The ENS computations imply the worse conditions rather than the base case.

Table 2. Energy surplus percentage of energy sources in EHP outage rather than base case.

Energy sources	EHP outage percentage		
	30%	50%	100%
CHP	1.03%	1.08%	1.14%
CB	1.01%	1.02%	1.04%
Furnace	1.06%	1.07%	1.11%
ESS	1.06%	1.08%	1.14%

When EHP is adjusted to be out of the circuit from the energy hub, the greatest pressure to the supply power will be applied to ESS and the CHP devices. This suggests that the unsupplied energy could increase by as much as 15%, which would result in a cost increase of approximately $3 million.

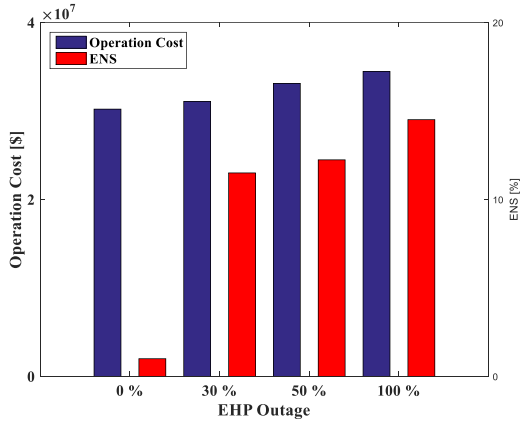

Figure 10. Operation costs and ENS in terms of EHP outage.

6.3. CB outage

The CB outage generally influences the cooling power that should be supplied. As shown in Table 3, the CB outage causes the ESS ice-making power to pressure to procure the cooling demand profile. Therefore, there are some ENS increments in this kind of energy required by the consumers. Figure 11 represents the operation costs and ENS in terms of the CB outage.

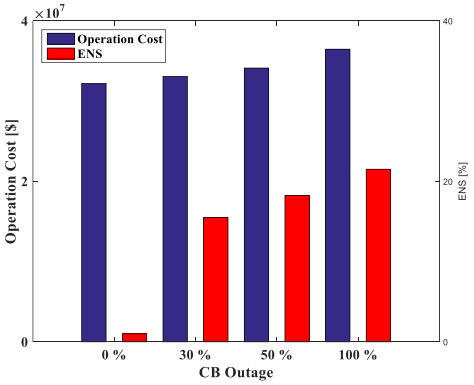

Figure 11. Operation costs and ENS in terms of CB outage.

Table 3. Energy surplus percentage of energy sources in CB outage rather than base case.

Energy sources	CB outage percentage		
	30%	50%	100%
CHP	1.07%	1.09%	1.17%
EHP	1.02%	1.05%	1.06%
Furnace	1.07%	1.08%	1.16%
ESS	1.12%	1.18%	1.25%

Since CB is used to supply the cooling load profiles, and there is not much alternative resource for it, if it goes out of the circuit, the amount of unsupplied energy will also increase sharply so that it is possible that approximately 23% of the total demand is not being supplied. Besides, the calculations show that the total cost of the operation and planning will increase by about $2.5 million in the case of CB outage.

6.4. Furnace outage

The furnace and CHP are the two important equipment to supply the thermal demand. Since the furnace is going to be out of the circuit, the CHP and ESS heating part have to supply the thermal power. Table 4 and figure 12 represent the output of the furnace outage.

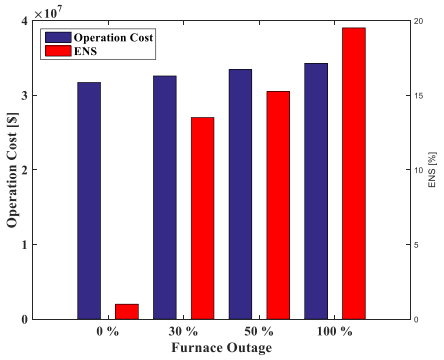

Figure 12. Operation costs and ENS in terms of furnace outage.

Table 4. Energy surplus percentage of energy sources in furnace outage rather than base case.

Energy sources	Furnace outage percentage		
	30%	50%	100%
CHP	1.13%	1.19%	1.28%
EHP	1.03%	1.06%	1.08%
CB	1.02%	1.04%	1.09%
ESS	1.13%	1.14%	1.20%

The furnace directly converts the energy received from the natural gas to heat, and plays an important role in supplying the thermal demand of the system. Therefore, if the furnace outage scenario is considered, it is possible that about 19% of the network loads will face a lack of energy. Correspondingly, in this case study, with the furnace outage from the energy hub circuit, the operating and planning costs will increase by $1.7 million, which is certainly not desirable.

6.5. ESS outage

Since the ESS equipment supplies both the electric and thermal powers (also the cooling power), the ESS outage will cause all devices to procure a lack load not supplied. Therefore, Table 5 and Figure 13 represent the ESS outage and its effect on the other energy sources, operation costs, and ENS.

Table 5. Energy surplus percentage of energy sources in ESS outage rather than base case.

Energy sources	Furnace outage percentage		
	30%	50%	100%
CHP	1.16%	1.22%	1.31%
EHP	1.09%	1.17%	1.28%
CB	1.10%	1.16%	1.29%
Furnace	1.17%	1.19%	1.30%

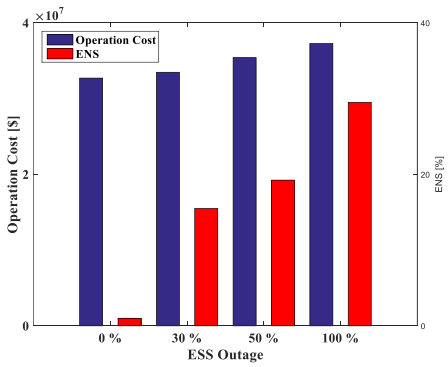

Figure 13. Operation costs and ENS in terms of ESS outage.

Since ESS plays an important role in providing the electrical, thermal, and cooling load profiles, its outage can have irreparable consequences on the system. The results shown in figure 13 show that in this case study, the unsupplied energy will reach about 28%, which will be more than the other studies studied. The operating costs will also increase by approximately $2.9 million. The minor changes in the price are due to the small capacity of the energy hub.

6.6. CVaR variations

In this section, it is assumed that the only factor that influences the ISO decisions is the conditional value at risk. The calculations show that the more risky the decisions made, a higher profit will be obtained. Table 6 explains the risk management variation in terms of the operation costs. Furthermore, Figure 14 shows the expected profit in terms of the risk factor increment from 0 to 5.

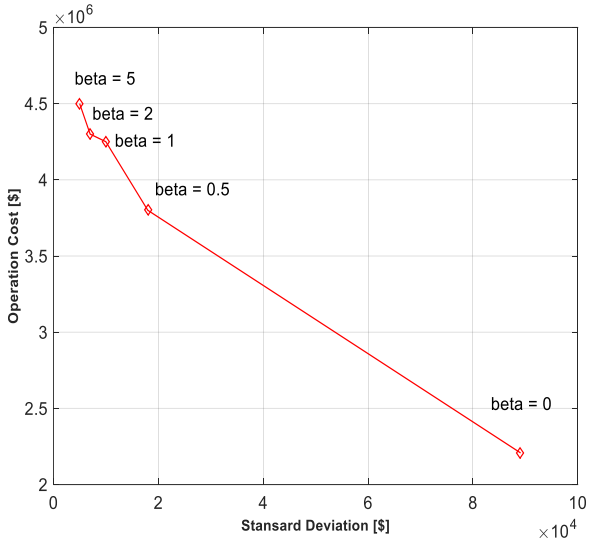

Figure 14. Expected profit in terms of risk factor increment.

The results shown in figure 14 represent that if the beta is reduced, the interest rate risk will increase, and they will earn higher profits. However, it is not without merit that the standard deviation of the profit also increases, which indicates that with changes in the reliability, there is a possibility of losing profit at higher risk levels. Table 6 shows that the lower the alpha, the lower the operating reliability, the company, and the futures contracts, and consequently, the higher the operating cost. Note that increasing the operating costs does not mean that the case study is undesirable, and will only be interpreted as one test of the total sensitivity analysis.

Table 6. Expected cost various risk factor variations.

		β				
		5	2	1	0.5	0
α	0.95	3.04e6	3.03e6	3.03e6	3.02e6	3.01e6
	0.85	3.04e6	3.04e6	3.03e6	3.02e6	3.01e6
	0.75	3.5e6	3.04e6	3.04e6	3.02e6	3.02e6

7. Conclusion

In this work, the sensitivity analysis of the operation scheduling in an energy hub system based on the natural gas, electric power, and thermal energy was investigated. The crisis management in this multi-carrier power grid showed that by choosing the correct share of input power carrier, the highest efficiency and the least cost could be achieved. The sensitivity analysis on the energy carriers such as CHP showed that the CHP power could be considered as the most efficient and profitable energy source since it had a low cost (about $3.012 million) in order to produce the electric and thermal powers simultaneously. The sensitivity analysis to reduce the consumption of natural gas showed that the operating cost would increase to about $3.235 million, and inevitably, a large percentage of the required thermal energy (about 18%) would have to be supplied by the electricity power directly, which is not desirable. If the total electric power is purchased from the upstream network, not only do the costs increase enormously but they also cause many power outages (about 24%) in the network, indicating that the power consumption is not satisfied. These phenomena will worsen the situation when the entire power grid is interrupted. At that time, only the electrical power on the grid is supplied by CHP, which causes it to turn into overload. The unsupplied energy in the scenarios considered, the more resources outflow, the higher the operating cost, and an unsupervised energy will be obtained. The worst case is when the consumed gas is out of the global grid as about 29%. The risk assessment is also an important factor in achieving a high profit for about $2.3 million (from $4.5 million to $2.2 million) by the independent operator, indicating the risk of choice. The conditional value at risk in the sensitivity analysis suggests that the higher the risk-taker of the future contract on the electricity market, the higher the gain, which, in turn, lowers the network's confidence. As a result, the sensitivity analysis is a major key in order to evaluate the grid load procurement performance under contingencies.

8. References

[1] R. Alayi, S. R. Seydnouri, M. Jahangeri, and A. Maarif, "Optimization, Sensitivity Analysis, and Techno-Economic Evaluation of a Multi-source System for an Urban Community: a Case Study." in Renewable Energy Research and Application, 2021.

[2] J. Nikoukar, S. Momen, and M. Gandomkar, "Determining the Optimal Arrangement of Distributed Generations in Micro-grids to Supply the Electrical and Thermal Demands using the Improved Shuffled Frog Leaping Algorithm." in Renewable Energy Research and Applications, 2021.

[3] S. M. Mirlohi, M. Sadeghzadeh, R. Kumar, and M. Ghassemieh, "Implementation of a Zero-energy Building Scheme for a Hot and Dry Climate Region in Iran (a Case Study, Yazd)." in Renewable Energy Research and Application, Vol. 1, No. 1, pp. 65-74, 2020.

[4] E. Mokaramian, H. Shayeghi, F. Sedaghati, A. Safari, and H. H. Alhelou, "A CVaR-Robust-Based Multi-objective Optimization Model for Energy Hub considering Uncertainty and E-Fuel Energy Storage in Energy and Reserve Markets," in IEEE Access, Vol. 9, pp. 109447-109464, 2021.

[5] J. Hu, X. Liu, M. Shahidehpour, and S. Xia, "Optimal Operation of Energy Hubs with Large-scale Distributed Energy Resources for Distribution Network Congestion Management," in IEEE Transactions on Sustainable Energy, vol. 12, no. 3, pp. 1755-1765, July 2021.

[6] M. Jadidbonab, B. Mohammadi-Ivatloo, M. Marzband, and P. Siano, "Short-term Self-scheduling of Virtual Energy Hub Plant Within Thermal Energy Market," in IEEE Transactions on Industrial Electronics, Vol. 68, No. 4, pp. 3124-3136, April 2021.

[7] S. Geng, M. Vrakopoulou, and I. A. Hiskens, "Optimal Capacity Design and Operation of Energy Hub Systems," in Proceedings of the IEEE, Vol. 108, No. 9, pp. 1475-1495, Sept. 2020.

[8] W. Zhong, C. Yang, K. Xie, S. Xie, and Y. Zhang, "ADMM-based Distributed Auction Mechanism for Energy Hub Scheduling in Smart Buildings," in IEEE Access, Vol. 6, pp. 45635-45645, 2018.

[9] M. Z. Oskouei, B. Mohammadi-Ivatloo, M. Abapour, M. Shafiee, and A. Anvari-Moghaddam, "Strategic Operation of a Virtual Energy Hub with the Provision of Advanced Ancillary Services in Industrial Parks," in IEEE Transactions on Sustainable Energy, Vol. 12, No. 4, pp. 2062-2073, Oct. 2021.

[10] P. Li, W. Sheng, Q. Duan, Z. Li, C. Zhu, and X. Zhang, "A Lyapunov Optimization-based Energy Management Strategy for Energy Hub with Energy Router," in IEEE Transactions on Smart Grid, Vol. 11, No. 6, pp. 4860-4870, Nov. 2020.

[11] Y. Luo, X. Zhang, D. Yang, and Q. Sun, "Emission Trading-based Optimal Scheduling Strategy of Energy Hub with Energy Storage and Integrated Electric Vehicles," in Journal of Modern Power Systems and Clean Energy, Vol. 8, No. 2, pp. 267-275, March 2020.

[12] L. Ma, N. Liu, J. Zhang, and L. Wang, "Real-time Rolling Horizon Energy Management for the Energy-Hub-Coordinated Prosumer Community from a Cooperative Perspective," in IEEE Transactions on Power Systems, Vol. 34, No. 2, pp. 1227-1242, March 2019.

[13] Y. Liang, W. Wei, and C. Wang, "A Generalized Nash Equilibrium Approach for Autonomous Energy Management of Residential Energy Hubs," in IEEE Transactions on Industrial Informatics, vol. 15, No. 11, pp. 5892-5905, Nov. 2019.

[14] I. G. Moghaddam, M. Saniei, and E. Mashhour, "A comprehensive model for self-scheduling an energy hub to supply cooling, heating, and electrical demands of a building," Energy, Vol. 94, pp. 157–170, 2016.

[15] A. Najafi, H. Falaghi, J. Contreras, and M. Ramezani, "Medium-term energy hub management subject to electricity price and wind uncertainty," Applied Energy, Vol. 168, pp. 418–433, Apr. 2016.

[16] A. Najafi, H. Falaghi, J. Contreras, and M. Ramezani, "A Stochastic Bilevel Model for the Energy Hub Manager Problem," IEEE Transactions on Smart Grid, Vol. 8, No. 5, pp. 2394–2404, Sep. 2017.

[17] X. Wang, N. Zhang, Z. Zhuo, C. Kang, and D. Kirschen, "Mixed-integer linear programming-based optimal configuration planning for energy hub: starting from scratch," Applied Energy, Vol. 210, pp. 1141–1150, Jan. 2018.

[18] A. Setlhaolo, S. Sichilalu, and J. Zhang, "Residential load management in an energy hub with heat pump water heater," Applied Energy, Vol. 208, pp. 551–560, Dec. 2017.

[19] A. Dolatabadi and B. Mohammadi-Ivatloo, "Stochastic risk-constrained scheduling of smart energy hub in the presence of wind power and demand response," Applied Thermal Engineering, Vol. 123, pp. 40–49, Aug. 2017.

[20] K. AlRafea, M. Fowler, A. Elkamel, and A. Hajimiragha, "Integration of renewable energy sources into combined cycle power plants through electrolysis-generated hydrogen in a new designed energy hub," International Journal of Hydrogen Energy, Vol. 41, No. 38, pp. 16718–16728, Oct. 2016.

[21] H. Ahmadisedigh and L. Gosselin, "Combined heating and cooling networks with waste heat recovery based on energy hub concept," Applied Energy, Vol. 253, p. 113495, Nov. 2019.

[22] R. Hemmati, "Stochastic energy investment in off-grid renewable energy hub for autonomous building," IET Renewable Power Generation, Vol. 13, No. 12, pp. 2232–2239, Sep. 2019.

[23] M. Rahmani-Andebili, "Stochastic, adaptive, and dynamic control of energy storage systems integrated with renewable energy sources for power loss minimization," Renewable Energy, Vol. 113, pp. 1462–1471, Dec. 2017.

[24] A. Maroufmashat, S. Sattari, R. Roshandel, M. Fowler, and A. Elkamel, "Multi-objective Optimization for Design and Operation of Distributed Energy Systems through the Multi-energy Hub Network Approach," Industrial and Engineering Chemistry Research, Vol. 55, No. 33, pp. 8950–8966, Aug. 2016.

[25] Y. Cao, W. Wei, J. Wang, S. Mei, M. Shafie-khah, and J. P. S. Catalao, "Capacity Planning of Energy Hub in Multi-carrier Energy Networks: a Data-driven Robust Stochastic Programming Approach," IEEE Transactions on Sustainable Energy, p 1, 2018.

[26] M.-W. Tian et al., "Risk-based stochastic scheduling of energy hub system in the presence of heating network and thermal energy management," Applied Thermal Engineering, Vol. 159, p. 113825, Aug. 2019